Estimation of hydrological response to future climate change in a cold watershed

Jian Sha, Zhong-Liang Wang, Yue Zhao, Yan-Xue Xu and Xue Li

ABSTRACT

The vulnerability of the natural water system in cold areas to future climate change is of great concern. A coupled model approach was applied in the headwater watershed area of Yalu River in the northeastern part of China to estimate the response of hydrological processes to future climate change with moderate data. The stochastic Long Ashton Research Station Weather Generator was used to downscale the results of general circulation models to generate synthetic daily weather series in the 2050s and 2080s under various projected scenarios, which were applied as input data of the Generalized Watershed Loading Functions hydrological model for future hydrological process estimations. The results showed that future wetter and hotter weather conditions would have positive impacts on the watershed runoff yields but negative impacts on the watershed groundwater flow yields. The freezing period in winter would be shortened with earlier snowmelt peaks in spring. These would result in less snow cover in winter and shift the monthly allocations of streamflow with more yields in March but less in April and May, which should be of great concern for future local management. The proposed approach of the coupled model application is effective and can be used in other similar areas.

Key words | climate change, hydrological process, model linkage, snowmelt, streamflow

Jian Sha
Zhong-Liang Wang (corresponding author)
Xue Li
Tianjin Key Laboratory of Water Resources and Environment,
Tianjin Normal University,
Tianjin 300387,
China
E-mail: *wangzhongliang@vip.skleg.cn*

Yue Zhao
Yan-Xue Xu
Water Environment Institute, Chinese Academy for Environmental Planning,
Beijing 100012,
China

INTRODUCTION

Water is a critical resource for human communities, with the vulnerability of water circulation and availability to the environment being of great concern (Stocker & Raible 2005; Oki & Kanae 2006). For regional security and sustainable development, it is important to realize the responses of hydrological processes to the changing environment at the watershed level (Milly *et al.* 2008). Regional climate change is one of the most significant factors that can directly affect local hydrological processes (Piao *et al.* 2010). On the one hand, precipitation is the source of water in rivers at the watershed outlet and its intensity and distribution have great impact on streamflow yields. On the other hand, the air temperature determines the precipitation's form and evapotranspiration during its transferred process in the watershed areas. Both the changes of precipitation and air temperature will potentially affect watershed hydrological processes and it is a great challenge to understand quantitatively how a changing climate status shifts original watershed water resource availability in different locations. The model approach is considered to be one of the most useful tools to address this issue (Cleridou *et al.* 2014).

Impact studies of the hydrological response to future climate change based on various models for quantitative estimation have been widely implemented worldwide (Bellin *et al.* 2016; Karlsson *et al.* 2016). Yan *et al.* (2016) assessed the combined impact of future climate and land use changes on streamflow using coupled model methods in the Xinjiang Basin of China. The average annual and seasonal variations of the surface and sub-surface hydrological processes in the Elbow River watershed area in Canada was

doi: 10.2166/wcc.2018.026

investigated under five GCM-scenarios up to 2070 using the physically-based, distributed MIKE SHE/MIKE 11 model (Farjad *et al.* 2016). The streamflow response to climate changes in the Luanhe River Basin in north China was investigated by Jiang *et al.* (2015), which was based on twenty hypothetical climate change scenarios with HIMS model simulations. Huyen *et al.* (2017) assessed the impacts of climate change on water resources in the Srepok watershed in the Central Highlands of Vietnam by using the Soil and Water Assessment Tool (SWAT) model based on A1B and A2 climate change scenarios in two future periods. A distributed hydrological soil vegetation model (DHSVM) was used to assess the effect of climate change on streamflow in the Tuotuo River basin, the source region of the Yangtze River, which was based on the results of Global Climate Models and downscaling outputs from the Long Ashton Research Station Weather Generator (LARS-WG) (Bian *et al.* 2017). Previous studies have indicated that the impact of changes in climate is critical for regional water resources.

Among various areas, the response of hydrological processes to future climate change in cold watersheds is of special concern (Musselman *et al.* 2017). Significant positive correlations between the changes of winter baseflow and mean annual air temperature have been detected, which resulted from the snowmelt and precipitation regime shifts that altered surface and subsurface hydrological processes (Duan *et al.* 2017a). Besides, there would be earlier flood peaks in spring and more low flow conditions during summer months due to the changes in the seasonal apportionment of annual water yields (Wijngaard *et al.* 2016). In addition, the possible impact of projected climate changes on streamflow was investigated in two snowmelt-dominated catchments located in the western and eastern regions of Canada using the SWAT hydrological model following the SRES A2 emissions scenario (Troin *et al.* 2015). Establishing proper approaches to estimating future watershed hydrological processes in cold conditions based on reliable model applications is of great significance.

In this study, we applied an integrated model linkage approach to estimate the responses of hydrological processes to modelled future climate change scenarios in a cold watershed area with moderate data requirements. A hydrological model of Generalized Watershed Loading Functions (GWLF) and a weather generator model of the LARS-WG were employed as the modelling tools, which had the advantage of having the potential capability to be coupled at the watershed level. Two future periods of the 2050s and 2080s based on three projected future emissions of A1B, A2 and B1 were estimated and compared with the baseline period of 1956–2015. The headwater watershed area of Yalu River in the northeast of China with cold weather conditions was set as the case study area and the responses of its hydrological processes to various projected future climate scenarios were estimated.

METHODS

Study area and data source

The headwater watershed area of Yalu River located in the northeastern area of China was the focus of this study (Figure 1). The Yalu River extends from the east side of Daxing'anling Mountains around Boketu town and drains into the Nen River, which is one of the main tributaries of the Songhua River. The portion of the Yalu River watershed located above Balin Hydrological Gauge Station was used as the study area with an area of about 2,851 km^2. The weather condition of the study area is cold with nearly a six month freeze-up period. It is a woodland-dominant upland watershed area with a mean elevation of 772 m, while its mean annual temperature and precipitation are −0.1 °C and 259 mm based on the records in the Boketu Meteorological Station, respectively. As one of the sources of Nen River, changes to the water resource property in Yalu River would be critical for regional water resources and farm activities in the Songnen plain, which are significant for local management.

The sources of original data used in this study mainly included basic watershed geographical information maps and historical observed data records. The general watershed attributes of river line and sub-watershed boundaries were generated from Arc Hydro Tools 2.0 by using a 90 m Digital Elevation Model (DEM) operated in the ArcGIS 10.2 platform. Land use types were classified based on China Current Land Use Classification (GB/T 21010-2007) into 25 sub-classifications. However, only 11 types occur in the

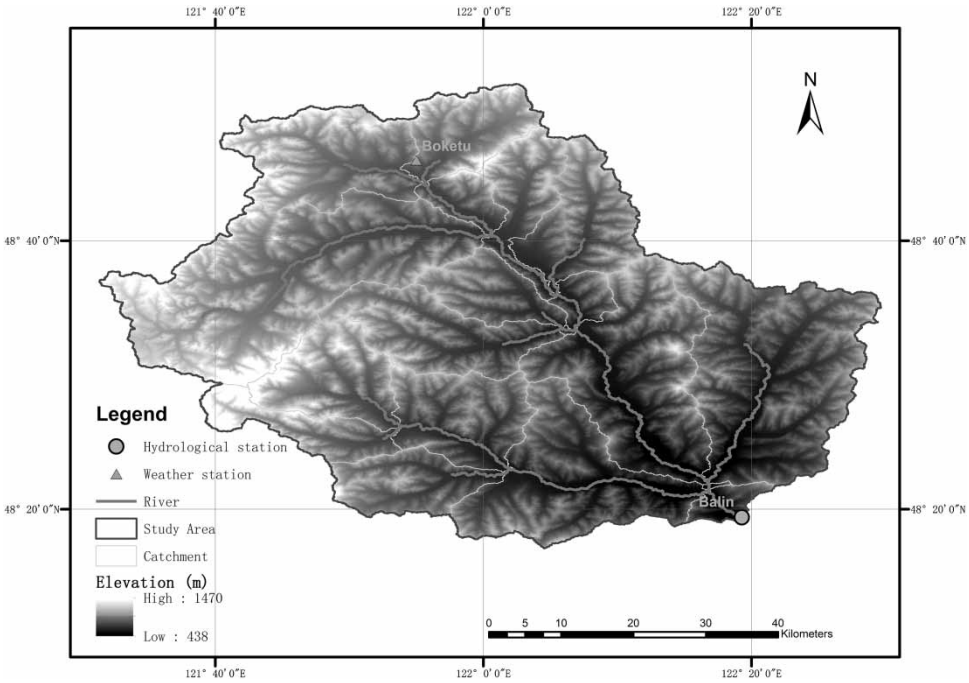

Figure 1 | Geographical location and watershed spatial attributes of the study area.

study region, the areas of which were calculated by Spatial Analyst Tools in ArcGIS 10.2 based on 1 km raster maps with percentages for each land use type. Observed minimum and maximum daily air temperatures and daily precipitation during 1956–2015 in the Boketu Meteorological Station were obtained from the National Meteorological Information Center of China. The hydrological data of monthly river flows in the Balin Hydrological Gauge Station were taken from the books of 'annual Hydrological Report P. R. China' in the period of 2009–2014 from the National Library of China. These data were used as model inputs and/or observed data for calibration or verification processes to support model applications.

Model descriptions

The GWLF model (Haith & Shoemaker 1987) was used to simulate and predict hydrological fluxes in the headwaters of the Yalu River. GWLF is a combined distributed and lumped parameter model that can estimate monthly water yields in rivers at the outlet of a watershed, called streamflow as model output. Based on the algorithm of GWLF, streamflow is made up of runoff and groundwater flow. The surface runoff framework of GWLF is generally considered to be distributed in the sense that it divides multiple homogenous land use areas based on the Soil Conservation Service Curve Number (SCS-CN) method. The sub-surface groundwater flow framework of GWLF is lumped with an integrated linear groundwater reservoir to describe shallow saturated sub-surface zones and calculate groundwater flow yields. The daily hydrological processes are estimated through a daily water balance approach and reliable monthly estimations can be calculated by ignoring the spatial routing of streamflow with the assumption that the travel times are considerably less than one month. In addition, a linear function in saturated process and a leakage coefficient in unsaturated process were added for better estimations in low-flow periods based on previous research (Sha *et al.* 2014). The GWLF is used here owing to its moderate data requirement that can be satisfied based on a basic public dataset in China. The Regional Nutrient Management (ReNuMa) software has the homologous hydrological algorithms as GWLF and it is employed here as a modeling tool for its flexible operation and great fitness at the scale of the study area (i.e. several thousand km^2 watershed). Besides, the Generalized Likelihood

Uncertainty Estimation (GLUE) procedure previously embedded in ReNuMa is operated for parameter calibrations and uncertainty estimations (Hong *et al.* 2012). The GWLF/ReNuMa model indicates reliable capability in estimations of watershed hydrological and/or hydrochemical processes with broad applications (Sharifi *et al.* 2017; Hu *et al.* 2018; Sha *et al.* 2018).

The statistical downscaling model named LARS-WG (Semenov & Barrow 1997) was used here for future weather data estimation. It uses a series of semi-empirical distributions to describe site-specific weather factors with various parameters, which are calibrated and validated based on long-time observed daily records that can be obtained in this study area. A synthetic time-series of daily precipitation and daily maximum and minimum temperatures can be generated by the calibrated LARS-WG through updating model parameters based on various GCM outputs. These synthetic time-series that represent different future changed climate status can be directly used in the GWLF model for future hydrological response estimations. The LARS-WG model has been widely used in the past decade for future climate estimations (Amin *et al.* 2014; Naderi & Raeisi 2016) and, with the benefits of its wet/dry series based approach for precipitation estimation, it offers great reliability when coupled with a watershed model for impact assessment of hydrological processes (Ayele *et al.* 2016; Danesh *et al.* 2016).

Three projected future emissions of A1B, A2 and B1 proposed by the Intergovernmental Panel on Climate Change (IPCC) in Fourth Assessment Report (AR4) were considered as climate change scenarios (Parry 2007). The A1B storyline describes a future world of very rapid economic growth, global population that peaks in mid-century and declines thereafter, and the rapid introduction of new and more efficient technologies with balanced energy sources. The A2 storyline describes a very heterogeneous world with self-reliance and preservation of local identities. The B1 storyline describes a convergent world with the same global population, which peaks mid-century and declines thereafter as in the A1 storyline, but with rapid change in economic structures toward a service and information economy, with reductions in material intensity and the introduction of clean and resource-efficient technologies. Although IPCC had released newer scenarios of representative concentration pathways (RCPS) based on a series of greenhouse gas concentration (not emissions) trajectories in the Fifth Assessment Report (AR5), these classic emissions-based scenarios in AR4 were still widely applied in recent research (Kim *et al.* 2017; Ojeda-Bustamante *et al.* 2017). The outputs of HADCM3 are used to update the model parameter of LARS-WG. The HADCM3 is one of the most popular global circulation models used in supporting estimations of hydrological response to climate change (Duan *et al.* 2017b; Nasseri *et al.* 2017) and its outputs facing various AR4 scenarios had been previously embedded into LARS-WG. Benefitting from the great links between HADCM and LARS-WG, the model parameters of LARS-WG could be feasibly updated to generate future synthetic site-scale daily weather data.

Model application

For the application of the GWLF model, the observed monthly streamflow records of 2009–2012 were used for calibration and the records of 2013–2014 were reserved for verification. The default range of GWLF parameters from the user manual were used as references to determine the prior distributions for each parameter. Based on this, 100,000 groups of model parameters were sampled, which was followed by the same number of model iterations to build up a reliable likelihood function distribution by comparing the modeled and observed values in the calibration period. The Nash–Sutcliff coefficient (R^2_{NS}) was used for measuring model accuracy, with the value of 0.85 set as the cutoff threshold for posterior sampling to describe the parameters' posterior distributions and results' uncertainties. The calibrated GWLF could be used to estimate future watershed hydrological statuses by replacing its weather input data with various synthetic time-series, which were modelled by LARS-WG in this subject.

For the application of the LARS-WG model, sixty years of observed daily weather records in the period of 1956–2015 in the Boketu meteorological station were first used to calibrate model parameters. The calibration process was automatically operated by LARS-WG and sixty years of synthetic daily weather data were then generated based on the calibrated model parameters with the alternative random

seed number of 4409, which were used for model validation by comparison with the observed daily weather records. The validated model parameters were updated based on three projected scenarios of A1B, A2 and B1 in two future periods of 2046–2065 (2050s) and 2080–2099 (2080s), and six groups of sixty years' synthetic daily weather data were generated to represent the future changed climate conditions.

Seven synthetic series of sixty years of daily weather data that indicated the current and future status were respectively used as the input weather data in the calibrated GWLF model for hydrological estimations, the results of which could be further compared and discussed to explore the watershed hydrological response to climate change impacts in this cold study area.

Table 1 | Results of the statistical tests comparing the observed data and synthetic data generated by LARS-WG with the numbers of tests revealing significant different results at 5% significance level

Items	Total tests	Number of significant difference	Percentage of significant difference (%)
WDSeries[a]	8	0	0.0
PrecD[b]	12	0	0.0
PMM[c]	12	1	8.3
PMV[d]	12	1	8.3
TminD[e]	12	0	0.0
TminM[f]	12	0	0.0
TmaxD[g]	12	0	0.0
TmaxM[h]	12	0	0.0

[a]Indicates seasonal wet/dry series distributions tested by the Kolmogorov–Smirnov (K–S) test.
[b]Indicates daily precipitation distributions tested by the Kolmogorov–Smirnov (K–S) test.
[c]Indicates monthly mean of precipitation tested by the t-test.
[d]Indicates monthly variances of precipitation tested by the F-test.
[e]Indicates daily minimum temperature distributions tested by the Kolmogorov–Smirnov (K–S) test.
[f]Indicates monthly mean of daily minimum temperature tested by the t-test.
[g]Indicates daily maximum temperature distributions tested by the Kolmogorov–Smirnov (K–S) test.
[h]Indicates monthly mean of daily maximum temperature tested by the t-test.

RESULTS AND DISCUSSION

Results of LARS-WG model

The observed and modelled daily weather data were compared through several statistical tests. The ratios of significant different results at the 5% significance level to the total number of tests were used to represent the model performance (Table 1). We found that most weather items had no significant differences between the observed and modelled datasets, indicating great modeling precision. The modelling ability of monthly precipitation and its variability were relatively poor with one significant different result for each. Assessing with graphic comparisons (Figure 2), the errors of precipitation simulations mainly occurred in the summer months with high precipitation, which is a common issue among statistical downscaling models including LARS-WG from its wet/dry-series based framework (Amin *et al.* 2014; Naderi & Raeisi 2016). The model performance was generally acceptable in supporting further scenario analysis with reliable synthetic weather data generations. A detailed parameter list of the LARS-WG model is provided in the supplementary material, available with the online version of this paper.

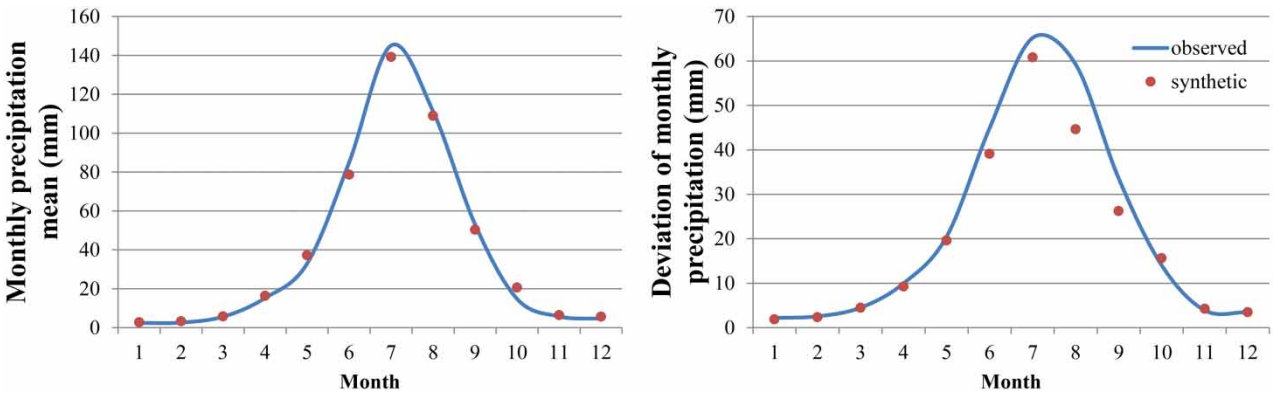

Figure 2 | Comparisons of the observed precipitations to the simulated values from LARS-WG on a monthly scale.

Results of GWLF model

The calibrated model parameters of GWLF are summarized in Table 2 and the modeled monthly streamflow were compared with the observed streamflow records during the research period (Figure 3). Both the R^2_{NS} and coefficient of determination in calibration period were 0.90, while the R^2_{NS} was 0.84 and the coefficient of determination was 0.85 in the validation period. The model results showed a great goodness-of-fit on streamflow simulations, indicating that the calibrated GWLF model could provide reliable estimations of the watershed hydrological responses towards future changed climate statuses, which are discussed in the next two sections.

Table 2 | Calibrated results of GWLF Hydrological parameters

		Bayesian posterior distributions	
Parameter items	**Subcategories**	**Mean**	**Standard deviation**
Runoff curve number	Cultivated land	47.52	13.55
	Wood land	21.36	6.13
	Sparsely forested woodland	24.57	7.04
	Other forest land including garden	32.81	9.52
	High coverage grassland	34.80	10.04
	Middle coverage grassland	51.80	14.86
	Low coverage grassland	59.03	16.71
	Water and wet land	99.89	25.23
	Exposed rock and shingle land	70.67	20.70
	Cities and towns	77.05	22.14
	Rural residential land	80.79	23.70
Evapotranspiration cover factor	JAN	0.50	0.14
	FEB	0.50	0.15
	MAR	0.51	0.15
	APR	0.49	0.14
	MAY	0.51	0.15
	JUNE	0.47	0.13
	JULY	0.56	0.14
	AUG	0.74	0.07
	SEPT	0.59	0.15
	OCT	0.50	0.14
	NOV	0.50	0.15
	DEC	0.50	0.14
Groundwater flow	Recession coefficient	0.0199	0.0047
	Seepage coefficient	0.0159	0.0045
	Recession slope (cm)	4.5814	1.3662
	Seepage slope (cm)	5.1830	1.3693
	Unsaturated zone leakage coefficient	0.2406	0.0703

Responses of annual hydrological processes

The changes in the watershed hydrological factors of streamflow, runoff, groundwater flow and evapotranspiration were estimated based on the output of GWLF. Seven groups of sixty years' synthetic daily weather data from the LARS-WG model outputs were used as the GWLF model inputs for scenario analysis. The watershed hydrological processes under current and future climate status were modeled and compared on an annual scale, the results of which are shown in Figure 4.

The results showed that due to future changed weather conditions, there is an increasing trend for runoff, but a decreasing trend for ground water flow. On one hand, the increases in annual runoff were different under different climate scenarios. The A2 scenario had the most significant impact on watershed runoff yields, under which the mean annual runoff would increase by 10.7% in the 2050s and even by 22.2% in the 2080s. The impact of the A1B scenario represented a rapid but non-persistent feature as the mean annual runoff would increase by 10.3% in the 2050s but only by 11.5% in the 2080s, reaching a steady state from the 2050s to 2080s. The B1 scenario showed a moderate impact in the near future as there was an increase of only 1.9% for the annual runoff in the 2050s, but a persistent effect existed with the mean annual runoff increasing by 12.6% in the 2080s, which is similar to that of the A1B scenario. On the other hand, there were also various behaviors of changes for the decreases in annual groundwater flow under different climate scenarios. The A2 scenario showed the least impact as the mean annual groundwater flow would only be decreased by 3.7% and 4.5% in the 2050s and 2080s, respectively. The A1B scenario had a significantly negative impact on the groundwater flow yields with the mean annual groundwater flow decreasing by 9.1% in the 2050s and even by 20.9% in the 2080s. The impact of the B1 scenario decreased initially and increased afterwards, under which the mean annual groundwater flow would be decreased by 21.6% in the 2050s before increasing. After this increase, the mean annual groundwater flow is lower by 6.5% in the 2080s compared to the baseline level. Furthermore, all three scenarios had positive impacts on

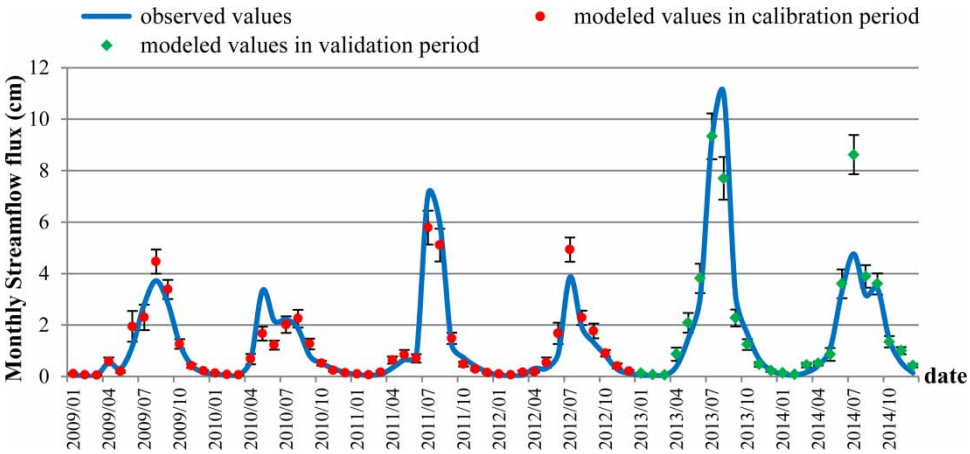

Figure 3 | Time series of observed and modeled monthly streamflow during the research period. The modelled values were the mean value of the posterior samples and the bars denoted the standard deviation.

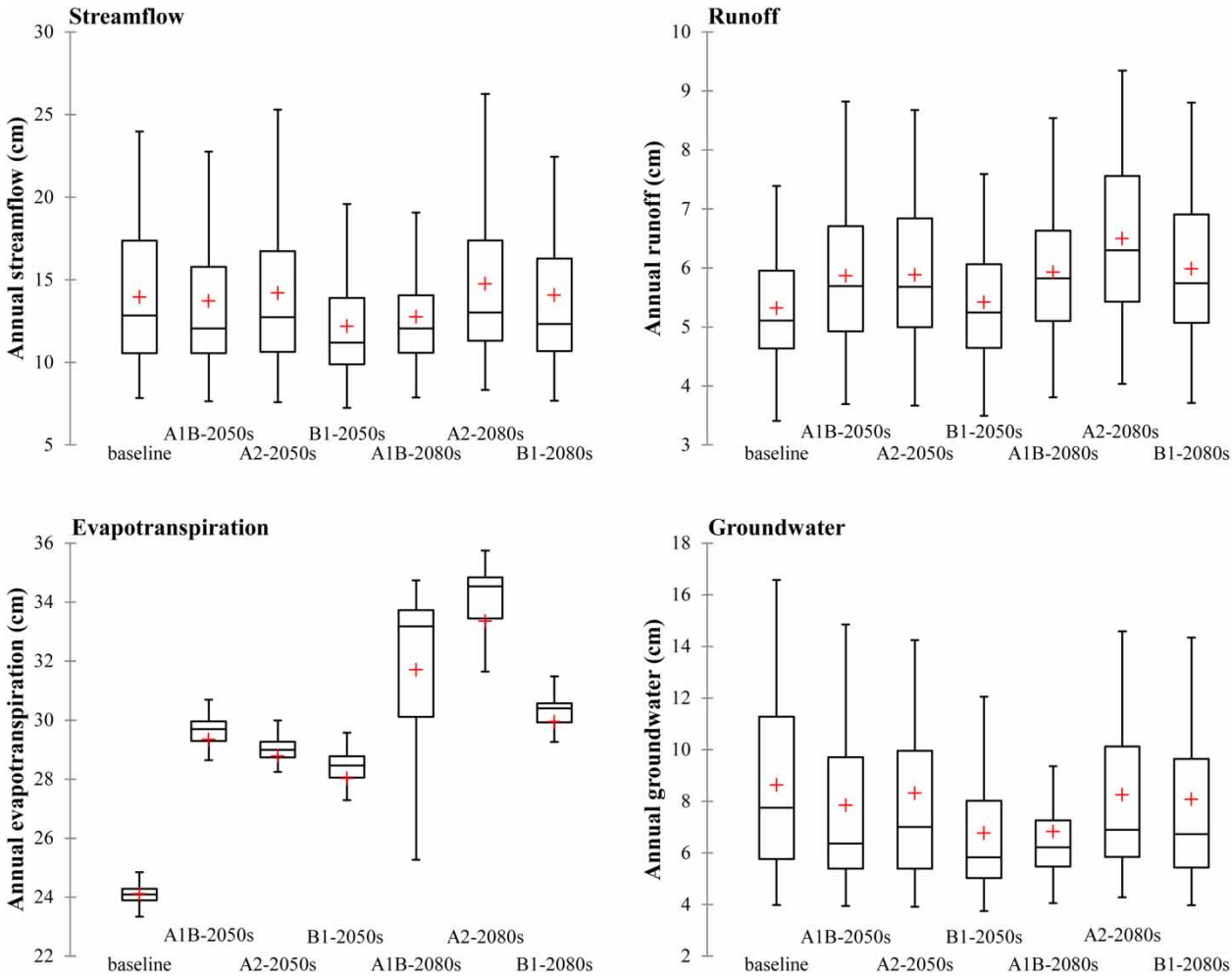

Figure 4 | The responses of hydrological processes in annual scale to future climate changes. The upper and lower border of the box represented the 25th and 75th percentiles; the line and cross in the box interior represented the median and mean values; and the 'whiskers' were the minimum and maximum values.

the evapotranspiration due to the hotter and wetter weather conditions in the future. In the 2050s, the A1B scenario had the largest impact as the mean annual evapotranspiration would be increased by 21.7%. In the 2080s, the A2 scenario had the largest impact as the mean annual evapotranspiration would be increased by 38.3%. The impact of the B1 scenario was the smallest in both future periods. There would also be more precipitation in future, which could offset the additional loss of water from evapotranspiration due to the higher temperatures. The watershed water transport process would also be changed, the results of which complicate the changes in future streamflow yields.

The responses of the annual streamflow under different climate scenarios are significantly diverse. The A1B scenario showed a negative impact as the mean annual streamflow would decrease by 1.7% in the 2050s and 8.6% in the 2080s. Conversely, the A2 scenario revealed a positive impact as the mean annual streamflow would increase by 1.8% in the 2050s and 5.7% in the 2080s. Under the B1 scenario, the mean annual streamflow would decrease by 12.6% initially in the 2050s but increase afterwards to reach the baseline level in the 2080s with a slight increase of 0.8%. In addition, the streamflow in extreme high flow years was examined. The top 10% highest annual streamflow for each scenario were defined as the extreme condition and their mean values were compared with the value in the baseline level. The results showed that most changing behaviors of the high annual streamflow were similar to that of the mean value, but had a greater increase under extreme conditions. The increase rates of extreme annual streamflows for the A2 scenario would be 7.2% in the 2050s and 7.9% in the 2080s, which are both higher than the results based on mean value statistics. The increase rates for B1 scenarios in the 2080s would be 6.8%, which is significantly higher than the mean-value-based rate. These results implied more flood risks during these future periods, which should be of great concern for local water source projects. Further, the changes in climate status would also convert the initial time distribution of watershed flow yields that is critical for management, which is detailed and discussed in the following section.

Changes in hydrological time distribution

The responses of monthly runoff, groundwater flow and streamflow to future changed climate conditions were estimated (Figure 5). The results showed that both the runoff

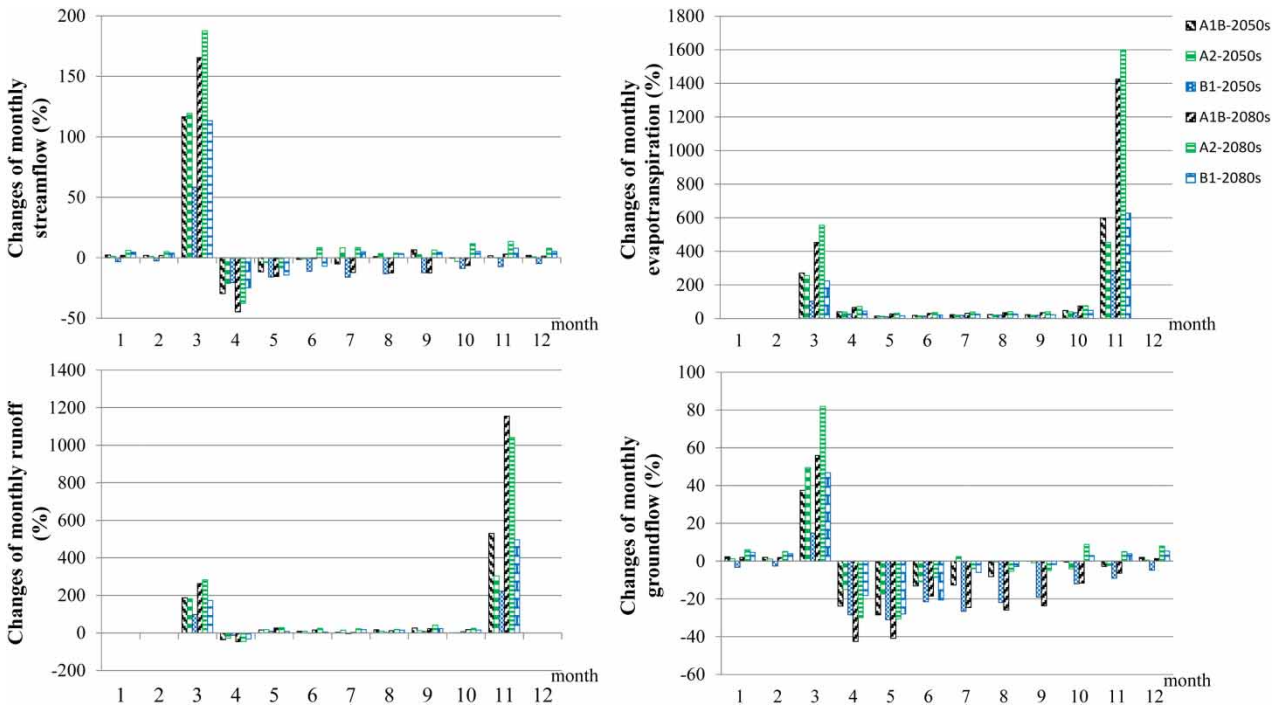

Figure 5 | The responses of main hydrological factors in future changed climate conditions.

and groundwater flow would be increased in March for all the climate scenarios and periods. Runoff also had a more significant increase in November together with several slight increases during May–October. Furthermore, there would be less runoff in April in the future and still no runoff yields in December, January and February due to the freezing conditions, which is the same as the baseline status. For groundwater flow, most future groundwater flows would be decreased in warm months during April–September. In addition, the changes in groundwater flows in the cold months of October–February would be generally slight, among which decreases were dominant in the 2050s but increases possibly occurred in the 2080s. As commonly determined by the runoff and groundwater flow processes, most of the changes in future monthly streamflow would mainly occur in spring. There would be significant increases in streamflow yields in March, which are consistent with the changes in runoff and groundwater flow. However, the streamflow yields would be decreased in April and May for all the projected future periods and climate scenarios. Most monthly streamflow yields in other months would be increased under the A2 scenario and decreased under the A1B and B1 scenarios, which are consistent with the changes in annual streamflow.

The changes in the hydrological process during spring mainly resulted from the higher temperature trends in the future, which would shorten the freeze period and influence the origin snow cover and snowmelt features. Benefits from the daily water balance framework of GWLF, the mean daily snow cover and snowmelt yields under the three climate scenarios in two future periods were estimated and compared with the baseline level (Figure 6). We found that there would be later trends for snow accumulation in autumn and earlier trends for snow thaw in spring in the future. Only the B1 scenario would have more snow cover during January–March than the baseline level, while all the other scenarios would lead to a decrease in snow cover accumulation during winter. The snowmelt in autumn under the baseline status mainly focused on October and its peak would happen around the 300th day of a year. However, under the future climate status, the peak of snowmelt in autumn would be advanced and the snow thaw would last even to November, which could lead to the decrease in snow cover accumulation. For the snow

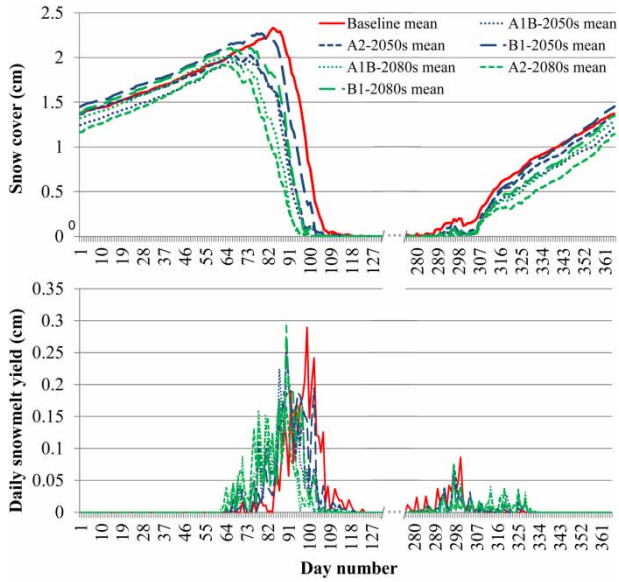

Figure 6 | Changes in mean daily snow cover and snowmelt yields in future climate conditions.

thaw in spring, the peak of snowmelt would also be advanced from around the 100th day for the baseline status to around the 85th day for the changed future climate status, which is probably the reason for the increases in March and decreases in April and May for the future monthly streamflow. These changes in streamflow distribution in time would be critical for local water resources and agricultural management as supporting information in decision-making.

CONCLUSIONS

This work modeled the response of hydrological processes to projected future climate scenarios with coupled applications of LARS-WG and GWLF and several conclusions were drawn from the results of the present study:

- There would be an increasing effect of the streamflow intensity in extreme high-flow years, though the changes in watershed streamflow would be different under various climate scenarios. More attention should be paid to risk control under extreme conditions for dam management of downstream reservoirs to ensure sensible water resource allocation and flood prevention.

- Future climate changes would shorten the freezing period and reduce snow cover accumulation, and lead to earlier snowmelt peaks and longer snow thawing periods. These changes of snow cover status in winter would affect the original mechanism of overwintering plant management and related measures should be designed. In addition, changed water resource allocation in spring should be considered for better regulation in order to meet the demands of cultivation in the downstream Songnen plain for spring wheat planting, which is one of the most important food crops in northeastern China.
- The hotter and wetter climate trends in the future would result in more runoff but less groundwater flow to make up the total watershed streamflow, indicating more water yields transferred through the surface approach. These changes would lead to a great potential risk of non-point source pollution and measures for runoff load reduction should be encouraged together with regional development, such as conservation tillage, terraces and diversions, and nutrient management to realize Best Management Practices (BMPs).
- The linkage application of LARS-WG and GWLF could achieve quantitative estimations of future hydrological processes under changed climate statuses and the coupled modeling approach proposed in this paper could be used as a tool for decision-making support in other similar watershed areas.

ACKNOWLEDGEMENTS

This work was supported by the Opening Fund of Tianjin Key Laboratory of Water Resources and Environment (117-YF11700102), Doctoral Fund of Tianjin Normal University (52XB1516), Tianjin Education Committee (TD13-5073), and National Natural Science Foundation of China (No. 41372373). The data set is provided by Climatic Data Center, National Meteorological Information Center, China Meteorological Administration (http://data.cma.cn), Geospatial Data Cloud site, Computer Network Information Center, Chinese Academy of Sciences (www.gscloud.cn), National Earth System Science Data Sharing Infrastructure, National Science & Technology Infrastructure of China (www.geodata.cn) and Data Center for Resources and Environmental Sciences, Chinese Academy of Sciences (RESDC) (www.resdc.cn). The authors acknowledge the developer of the ReNuMa and LARS-WG for free access to the software, code, and license agreement. The authors would also like to acknowledge Prof. Yuqiu Wang and his research team in Nankai University for their previous contributions concerning GWLF.

REFERENCES

Amin, M. Z. M., Islam, T. & Ishak, A. M. 2014 Downscaling and projection of precipitation from general circulation model predictors in an equatorial climate region by the automated regression-based statistical method. *Theor. Appl. Climatol.* **118** (1), 347–364.

Ayele, H. S., Li, M. H., Tung, C. P. & Liu, T. M. 2016 Assessing climate change impact on Gilgel Abbay and Gumara Watershed Hydrology, the Upper Blue Nile Basin, Ethiopia. *Terr. Atmos. Ocean. Sci.* **27** (6), 1005–1018.

Bellin, A., Majone, B., Cainelli, O., Alberici, D. & Villa, F. 2016 A continuous coupled hydrological and water resources management model. *Environ. Model. Softw.* **75**, 176–192.

Bian, H., Lü, H., Sadeghi, A., Zhu, Y., Yu, Z., Ouyang, F., Su, J. & Chen, R. 2017 Assessment on the effect of climate change on streamflow in the source region of the Yangtze River, China. *Water* **9** (1), 70.

Cleridou, N., Benas, N., Matsoukas, C., Croke, B. & Vardavas, I. 2014 Water resources of Cyprus under changing climatic conditions: modelling approach, validation and limitations. *Environ. Model. Softw.* **60**, 202–218.

Danesh, A. S., Ahadi, M. S., Fahmi, H., Nokhandan, M. H. & Eshraghi, H. 2016 Climate change impact assessment on water resources in Iran: applying dynamic and statistical downscaling methods. *J. Water Clim. Change* **7** (3), 551–577.

Duan, L., Man, X., Kurylyk, B. & Cai, T. 2017a Increasing Winter baseflow in response to permafrost thaw and precipitation regime shifts in northeastern China. *Water* **9** (1), 25.

Duan, W., He, B., Takara, K., Luo, P., Nover, D. & Hu, M. 2017b Impacts of climate change on the hydro-climatology of the upper Ishikari river basin, Japan. *Environ. Earth Sci.* **76** (14), 490.

Farjad, B., Gupta, A. & Marceau, D. J. 2016 Annual and seasonal variations of hydrological processes under climate change scenarios in two sub-catchments of a complex watershed. *Water Resour. Manage.* **30** (8), 2851–2865.

Haith, D. A. & Shoemaker, L. L. 1987 Generalized watershed loading functions for stream flow nutrients. *J. Am. Water Resour. Assoc.* **23** (3), 471–478.

Hong, B., Limburg, K. E., Hall, M. H., Mountrakis, G., Groffman, P. M., Hyde, K., Luo, L., Kelly, V. R. & Myers, S. J. 2012

An integrated monitoring/modeling framework for assessing human–nature interactions in urbanizing watersheds: Wappinger and Onondaga Creek watersheds, New York, USA. *Environ. Model. Softw.* **32**, 1–15.

Hu, M., Liu, Y., Wang, J., Dahlgren, R. A. & Chen, D. 2018 A modification of the Regional Nutrient Management model (ReNuMa) to identify long-term changes in riverine nitrogen sources. *J. Hydrol.* **561**, 31–42.

Huyen, N. T., Tu, L. H., Tram, V. N. Q., Minh, D. N., Liem, N. D. & Loi, N. K. 2017 Assessing the impacts of climate change on water resources in the Srepok watershed, Central Highland of Vietnam. *J. Water Clim. Change* **8** (3), 524–534.

Jiang, Y., Liu, C. & Li, X. 2015 Hydrological impacts of climate change simulated by HIMS models in the Luanhe River Basin, North China. *Water Resour. Manage.* **29** (4), 1365–1384.

Karlsson, I. B., Sonnenborg, T. O., Refsgaard, J. C., Trolle, D., Børgesen, C. D., Olesen, J. E., Jeppesen, E. & Jensen, K. H. 2016 Combined effects of climate models, hydrological model structures and land use scenarios on hydrological impacts of climate change. *J. Hydrol.* **535** (Supplement C), 301–317.

Kim, Y. D., Kim, J. M. & Kang, B. 2017 Projection of runoff and sediment yield under coordinated climate change and urbanization scenarios in Doam dam watershed, Korea. *J. Water Clim. Change* **8** (2), 235–253.

Milly, P. C. D., Betancourt, J., Falkenmark, M., Hirsch, R. M., Kundzewicz, Z. W., Lettenmaier, D. P. & Stouffer, R. J. 2008 Stationarity Is dead: whither water management? *Science* **319** (5863), 573–574.

Musselman, K. N., Clark, M. P., Liu, C. H., Ikeda, K. & Rasmussen, R. 2017 Slower snowmelt in a warmer world. *Nat. Clim. Chang.* **7** (3), 214–219.

Naderi, M. & Raeisi, E. 2016 Climate change in a region with altitude differences and with precipitation from various sources, South-Central Iran. *Theor. Appl. Climatol.* **124** (3), 529–540.

Nasseri, M., Zahraie, B. & Forouhar, L. 2017 A comparison between direct and indirect frameworks to evaluate impacts of climate change on streamflows: case study of Karkheh River basin in Iran. *J. Water Clim. Change* **8** (4), 652–674.

Ojeda-Bustamante, W., Ontiveros-Capurata, R. E., Flores-Velázquez, J. & Iñiguez-Covarrubias, M. 2017 Changes in water demands under adaptation actions to climate change in an irrigation district. *J. Water Clim. Change* **8** (2), 191–202.

Oki, T. & Kanae, S. 2006 Global hydrological cycles and world water resources. *Science* **313** (5790), 1068–1072.

Parry, M. L. 2007 *Climate Change 2007 – Impacts, Adaptation and Vulnerability: Working Group II Contribution to the Fourth Assessment Report of the IPCC*. Cambridge University Press, Cambridge, UK, pp. 469–506.

Piao, S., Ciais, P., Huang, Y., Shen, Z., Peng, S., Li, J., Zhou, L., Liu, H., Ma, Y., Ding, Y., Friedlingstein, P., Liu, C., Tan, K., Yu, Y., Zhang, T. & Fang, J. 2010 The impacts of climate change on water resources and agriculture in China. *Nature* **467** (7311), 43–51.

Semenov, M. A. & Barrow, E. M. 1997 Use of a stochastic weather generator in the development of climate change scenarios. *Clim. Change* **35** (4), 397–414.

Sha, J., Wang, Z.-L., Lu, R., Zhao, Y., Li, X. & Shang, Y.-T. 2018 Estimation of the source apportionment of phosphorus and its responses to future climate changes using multi-model applications. *Water* **10** (4), 468.

Sha, J., Swaney, D. P., Hong, B., Wang, J., Wang, Y. & Wang, Z.-L. 2014 Estimation of watershed hydrologic processes in arid conditions with a modified watershed model. *J. Hydrol.* **519**, 3550–3556.

Sharifi, A., Yen, H., Boomer, K. M. B., Kalin, L., Li, X. & Weller, D. E. 2017 Using multiple watershed models to assess the water quality impacts of alternate land development scenarios for a small community. *CATENA* **150**, 87–99.

Stocker, T. F. & Raible, C. C. 2005 Climate change: water cycle shifts gear. *Nature* **434** (7035), 830–833.

Troin, M., Velázquez, J. A., Caya, D. & Brissette, F. 2015 Comparing statistical post-processing of regional and global climate scenarios for hydrological impacts assessment: a case study of two Canadian catchments. *J. Hydrol.* **520** (Supplement C), 268–288.

Wijngaard, R. R., Helfricht, K., Schneeberger, K., Huttenlau, M., Schneider, K. & Bierkens, M. F. P. 2016 Hydrological response of the Ötztal glacierized catchments to climate change. *Hydrol. Res.* **47** (5), 979–995.

Yan, R., Huang, J., Wang, Y., Gao, J. & Qi, L. 2016 Modeling the combined impact of future climate and land use changes on streamflow of Xinjiang Basin, China. *Hydrol. Res.* **47** (2), 356–372.

First received 23 January 2018; accepted in revised form 9 June 2018. Available online 5 July 2018